Lightweight Components Manufactured with In-Production Composite Scraps: Mechanical Properties and Application Perspectives

(Article begins on next page)

28 April 2024

Lightweight components manufactured with in-production composite scraps: mechanical properties and application perspectives

D. Fiumarella, G. Belingardi, S. Boria, V. Castorani, A. Nardinocchi, A. Scattina

Abstract

In the last years, the design in the automotive sector is mainly led by emission reduction and circular economy. To satisfy the first perspective, composites materials are being increasingly used to produce lightweight structural and semi-structural components. However, the automotive mass production arises the problem of the end-of-life disposal of the vehicle and the reduction of the wastes environmental impact. The circular economy of the composite materials has therefore become a challenge of primary importance for car manufacturers and tier 1 suppliers. It is necessary to pursue a different economic model, combining traditional raw materials with the intensive use of materials from recycling processes. New technologies are being studied and developed concerning the reuse of in-line production scraps with out-of-autoclave process that makes them desirable for high production rate applications.

In this frame, a methodology for the reuse of prepreg cutouts coming from in-line ply cutting process is proposed. Production cutouts (scraps, or chops) are used as a charge to manufacture components through the compression molding process. The structure of the final part keeps in meso-scale the same orthotropic orientation of the chops, although it is quasi-isotropic from a macroscopic point of view. Accordingly, standard three-point bending, and tensile mechanical tests were performed to characterize the mechanical behavior of the material.

Failure modes and fracture propagation were analyzed too. The chop interface resulted to affect the mechanical performance. Before material failure, multiple damage precursor sites nucleated, generally in correspondence of the chop interfaces. Delamination, brittle fracture of the matrix and debonding between the chops were the main failure modes. The results of the standard coupon tests evidenced good performance of the material in terms of strength and stiffness, despite lower than standard 2x2 twill structure, making the studied material suitable for semi-structural purposes. Accordingly, a prototype of an accelerator pedal frame was produced, in order to evaluate the feasibility, the potential limitations and the aspects to be optimized for the manufacturing of a more complex component.

1. Introduction

The fuel consumption and pollutant emission reductions represent important aspects to be pursued by the automotive industry. The vehicle weight reduction is still a very effective way of cut off the fuel consumption and, as a consequence, the generation of greenhouse gases too. It has been estimated that, over a year, a 7% fuel saving is obtained for every 10% of the weight reduced from the total car weight. To produce even lighter structures without the need of compensate for any performance reduction, car manufacturers are replacing conventional materials, such as steel and aluminum, with polymeric composite materials [1]. It is well known that structural composite materials have mechanical characteristics similar to the metallic ones, but they have the advantage of being lighter. A number of structural elements (frame, hood, roof lining, doors and tailgate, bumpers, dashboard, cross member, suspension arms, seat frame, engine subframe, battery support trellis, etc.) can be produced by using several specific technologies, including composite materials based on bidirectional fiber fabrics systems, to ensure high mechanical performance.

Furthermore, the automotive mass production arises the problem of the end of life dismiss of the vehicle and the reduction of the wastes environmental impact. The European directive 2000/53 / EC [2] states that all the car manufacturers must strictly respect the reusability and recyclability standards for their products. The 95% of the car's weight must be made up from recoverable materials. Specifically, the 85% through the

recovery of the material or the reuse of components and the 10% through energy recovery. The circular economy of the composite materials has therefore become a challenge of primary importance for the automotive sector. It is necessary to pursue a different economic model, combining traditional raw materials with the intensive use of materials from recycling processes. The systematic waste disposal along the entire value chain, including the production stage represents a challenging target to get.

New technologies are being studied and developed concerning both the recycling of end-of-life composite products [3–8] (i.e., implementing thermoplastic fiber reinforced composites [9–12]) and the reuse of in-line production scraps. This last target can be achieved by a wide implementation of the stochastic prepreg platelet molded composites (PPMC).

The PPMCs or chopped composites are materials obtained by cutting prepreg tapes into chops of a defined dimension. Chops are submitted to a compression molding process. The orientation of these chops is uncontrolled during the compression molding process, and the output structure presents a random orientation of the chops. This stochastic structure translates into uncertain and scattered properties of the material that needs extensive experimental characterization to predict a distribution within the results can most likely be encompassed. Several studies on the experimental characterization of the unidirectional prepreg molded composites [13–17] demonstrated that this kind of structure presents lower mechanical properties compared to the continuous fiber composites. However, the possibility of produce composite parts with out-of-autoclave process makes them desirable for high production rate applications. Indeed, the authors of [18,19] produced complex randomly oriented unidirectional strand composite parts with variable thickness and rib features and investigated the effect of the process conditions on the quality of the product.

Concerning the automotive industry, carbon fiber composites with 2x2 fabric structure currently find wider application than the unidirectional fibers. Due to the high volume of prepreg scraps produced every year, the PPMC technology can contribute to drastically reduce the wastes. However, to the authors knowledge, only few works are present in literature concerning the study of the mechanical properties and the production process of PPMCs produced with bidirectional 2x2 prepreg scraps.

In this work, a methodology for the reuse of prepreg cutouts coming from in-line ply cutting process is proposed. Production cutouts (scraps, or chops) are used as a charge to manufacture components through the compression molding process. The structure of the final component keeps in meso-scale the same orthotropic fiber orientation of the chops, although it is quasi-isotropic from a macroscopic point of view. Standard mechanical tests were performed to characterize the behavior of the material. The results of the experimental tests evidenced good performance of the obtained material in terms of resistance and stiffness, despite lower than the standard 2x2 twill material, making the chopped composite material suitable for semi-structural purposes. Accordingly, failure modes and fracture propagation were analyzed. Chop interface resulted to affect the mechanical performances. Before material failure, multiple damage precursor sites nucleated, generally in correspondence of the chop interfaces. Delamination, brittle fracture of the matrix and debonding between the chops were the main failure modes.

Finally, a first prototype of an pedal accelerator frame was produced too, in order to evaluate the feasibility, the potential limitations and the design variables to account for the manufacturing of a more complex component, that will be deepened by the authors in future works.

2. Material and method

2.1 Production process

The material used was a 2x2 twill carbon fiber and epoxy resin prepreg. Two prepreg densities were used to produce the specimens to be tested: 204 g/m^2 and 600 g/m^2. The plates from which the specimens were

waterjet cut were produced by compression molding. Randomly oriented prepreg cuts (chops) were used as the thermoforming charge. The flat mold had a size of 350x350cm and a closing gap of 2.6 mm.

The production process is shown in figure 1. The uncured prepreg was cut into square chops of equal size each (20 mm of side). The prepreg scraps were placed in the freezer for about 20 minutes, to allow for easy detachment during the deposition stage. Subsequently, the chops were evenly distributed on the bottom mold surface (figure 1b), that was preheated to 100°C. Then the mold was closed, and the temperature was raised to 140°C. Once this temperature was reached, a pressure of 23 bar was applied, and these conditions were kept for 90 minutes. Picture of Figure 1c shows the plate produced by thermoforming: it is possible to appreciate the discontinuous and random orientation of the fibers. Compared to a short fiber composite, in which each fiber is oriented in a different way, in this case each chop locally retains its orthotropic structure.
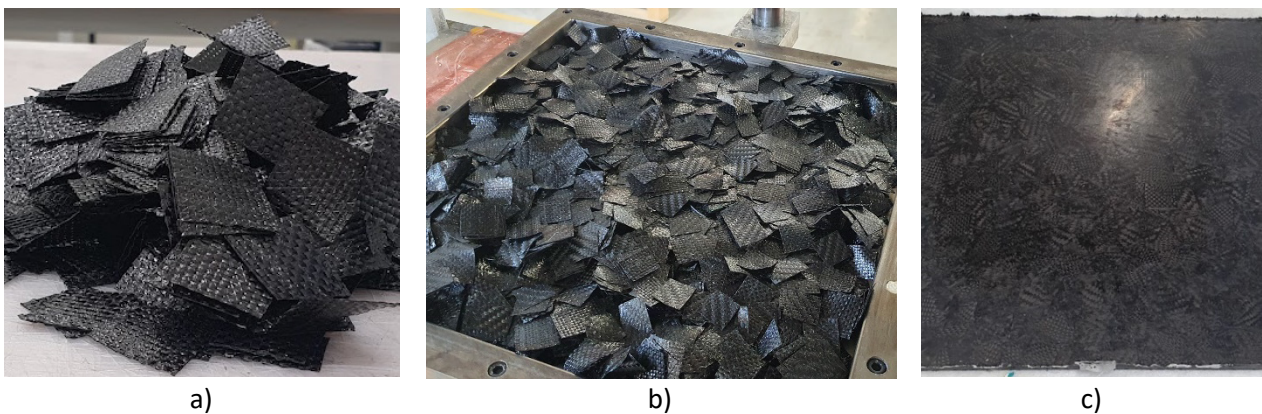

a)   b)   c)

Figure 1. Plate production process: a) prepreg chops cut; b) chops deposition on the mold; c) final component

2.2 Experimental Test

An experimental campaign was carried out to characterize the properties of the chopped composite. Tensile test and three point bending test were performed on specimens produced with both the prepreg densities (600 gr/m^2 and 204 gr/m^2). The tests were carried out in the testing laboratory of the Politecnico di Torino using an Instron servo-hydraulic universal material testing machine. Figure 2a shows the three-point bending test set-up. Two adjustable cylindrical pins were used as support span, and the specimen was loaded with a cylindrical steel head, fixed to the hydraulic grips of the testing machine, and centered with respect to the support span.

The tensile test set-up is shown in figure 1b. The specimen was constrained on both sides to the test machine. The tensile specimens were painted white, and a black paint pattern was created using an airbrush, to evaluate the deformation gradient through the Digital Image Correlation (DIC) system.

The standard three point bending test were executed according to the ASTM D790, and the tensile tests according to the ASTM D3039.

The size effect of this kind of structure was investigated, as the ratio between the specimen size to the chop size can strongly influence the mechanical properties [20]. Accordingly, specimens of different sizes respect to the ones suggested by the standard were tested both in bending (table 1, specimens F1-F6, in this case only the 204 gr/m^2 density was tested) and in tension (table 2, specimens T1). An 1:16 ratio between the specimen thickness and the span was considered for all the bending specimen dimensions. The gauge length used in the tensile tests was set to 158 mm for the Ts specimens (table 2) according to the standard. T1 specimens were shorter than Ts ones, and the gauge length imposed was equal to 57 mm.

Figure 2. Experimental tests set-up: a) three point bending test; b) tensile test.

Table 1. Bending specimen properties

Specimen name	Width [mm]	Thickness [mm]	Span [mm]
Fs	12.7		
F1	18		
F2	20		
F3	22	2.7	43
F4	25		
F5	30		
F6	33		

Table 2. Tensile specimen properties

Specimen name	Width [mm]	Gauge [mm]	Thickness [mm]
Ts	25	158	2.7
T1	13	57	

3. Results and discussion

3.1 Three point bending test

Figure 3 shows the three point bending test results carried out on the standard specimens. The results are normalized according to the maximum values of strength and Young modulus found in the batch of the tested specimen. Specimen with the prepreg density of 204 gr/m^2 performed better than the 600 gr/m^2 ones in terms of strength. From figure 3a it is possible to appreciate that the mean strength value of the 204 gr/m^2 specimens is considerably higher than the 600 gr/m^2 specimens. Furthermore, for these specimens, the dispersion of the strength results is higher respect to the 204 gr/m^2 coupons. Indeed, the normalized standard deviation of the 204 gr/m^2 specimens was 0.127 against 0.135 of the 600 gr/m^2 specimens, both values are in the acceptability range. Considering the Young Modulus (figure 3b), the mean value of the 204 gr/m^2 and the 600 gr/m^2 specimens are comparable. In this case, the result dispersion is remarkable both for 204 gr/m^2 and 600 gr/m^2 specimens. The high result dispersion can be explained by analyzing the fracture and failure modes of the tested specimens.
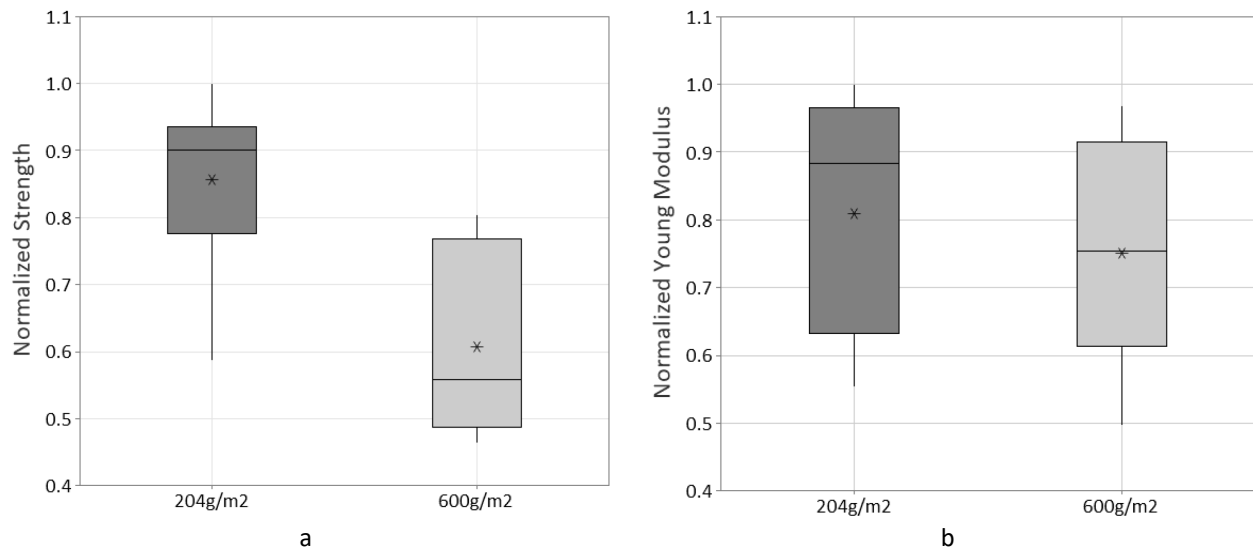
Figure 3. Box plot of the bending test results. a) Normalized strength; b) normalized Young modulus. Data are divided according to the prepreg densities. The asterisk represents the data mean; the horizontal line represents the data median.

Figure 4 shows the bending test results of the standard specimens in terms of the force-displacement trend. The loads were normalized as a function of the maximum force value measured in the tests. For clarity and readability, only some curves of the tested batch have been inserted in the graph. The high degree of the material inhomogeneity causes result dispersion in terms of stiffness, and the maximum load results are scattered too due to the different crack nucleation and propagation modes. It is possible to distinguish two different types of post-linear behavior (figure 4b): type 1) propagation and delamination, and type 2) quasi-brittle failure. The discriminant between these two behaviors is the initial nucleation point of the fracture.

Analyzing the material in a mesoscopic scale, it can be divided into two main structures: the orthotropic regions and the interface regions. The orthotropic regions are material portions where the prepreg chops keep their pristine structure, and thus the local fiber volume fraction (FVF) locally corresponds to the virgin prepreg FVF. The interface regions are transition areas between one chop and another. Here, the FVF is lower than the pristine prepreg, and the fibers form a swirl path. The interface regions represent a material discontinuity, where stresses can concentrate, and thus, according to their position and orientation, they can highly influence the material mechanical response.

Considering the type 1 specimens, the crack nucleates and propagates starting from the interface regions of the chops (figure 4b). The primary fracture occurs in correspondence of the transition area between two chops (interface region), far from the load application section (i.e., the point that carries the higher load). Due to the discontinuity of the interface regions, stresses redistribute near these zones, where the properties are matrix-dominant due to the high concentration of resin. As soon as the crack extends along the entire interface region, moving along the y direction (figure 4b), the delamination starts to propagate in the x direction (figure 4b). During this stage, a step-like trend of the force occurred, similarly to what happen in a single leg bending test, where the crack is loaded in a mixed way (mode 1 and mode 2) [21,22]. Considering the type 2 fracture behaviour, fiber rupture caused the failure in proximity of the surface of the load application point. The crack propagated in the z direction, and no delamination occurred (figure 4b).
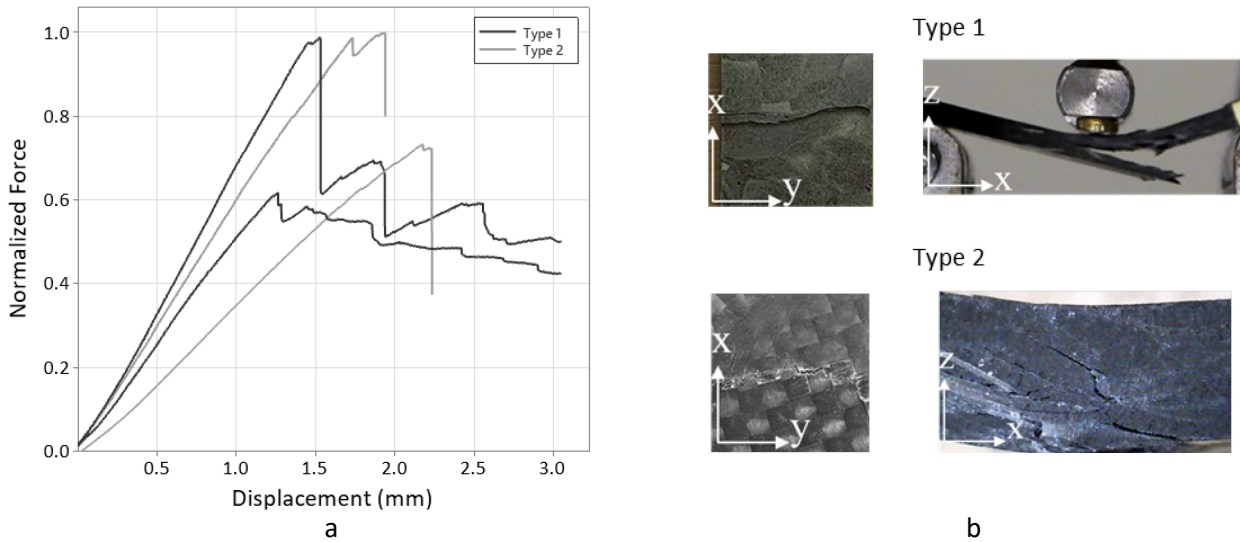
Figure 4. Three point bending test results. a) Normalized force trend vs displacement; b) fracture surfaces. Type 1 and type 2 represents the two failure modes.

Figure 5 shows the results of the flexural tests performed on the non-standard specimens at different widths. The values of the stress and the bending modulus are normalized as a function of the maximum stress value and the maximum bending modulus evaluated in the tests.

As can be noticed from figure 5b, an increase in the width from 12.7 mm to 25 mm, corresponds to a relative decrease in the flexural elasticity modulus. The modulus of the specimen F4 (25 mm of width) is the 60% lower than the modulus evaluated for the standard specimens Fs (12.7 mm of width). The strength slightly increases from 12.7 mm to 18 mm, even if a further increase of the width leads the maximum resistance value to sharply drop down until a minimum, in correspondence of 25 mm of width. Both the minimum of Young modulus and strength were found for the F4 specimens (25 mm of width): after this value, a trend reversal can be appreciated in both the charts (figure 5a and 5b). However, the size effect seems to have a greater impact on the maximum resistance value rather than on the stiffness. This effect is due to the peculiar material structures, where different fracture modes can be obtained.

Considering the specimen's widths from 18 to 25 mm the fracture propagated along the interface line between two chops. The crack nucleated from one edge and then propagated following the interface line, until it reached the opposite edge. After that, delamination occurred, and the failure is dominated by the type 1 fracture (figure 4a). On the other hand, considering the specimen's widths from 30 to 33 mm, the strength was considerably higher than smaller coupons. In this case, the width of the specimen is greater than the nominal width of the chop, and the crack encountered various resistance zones along its path (i.e., another chop oriented in a different way, or interface regions between the chops perpendicular to the direction of propagation) leading to an increase of the fracture propagation resistance. For these specimens, a type 2 failure occurred.
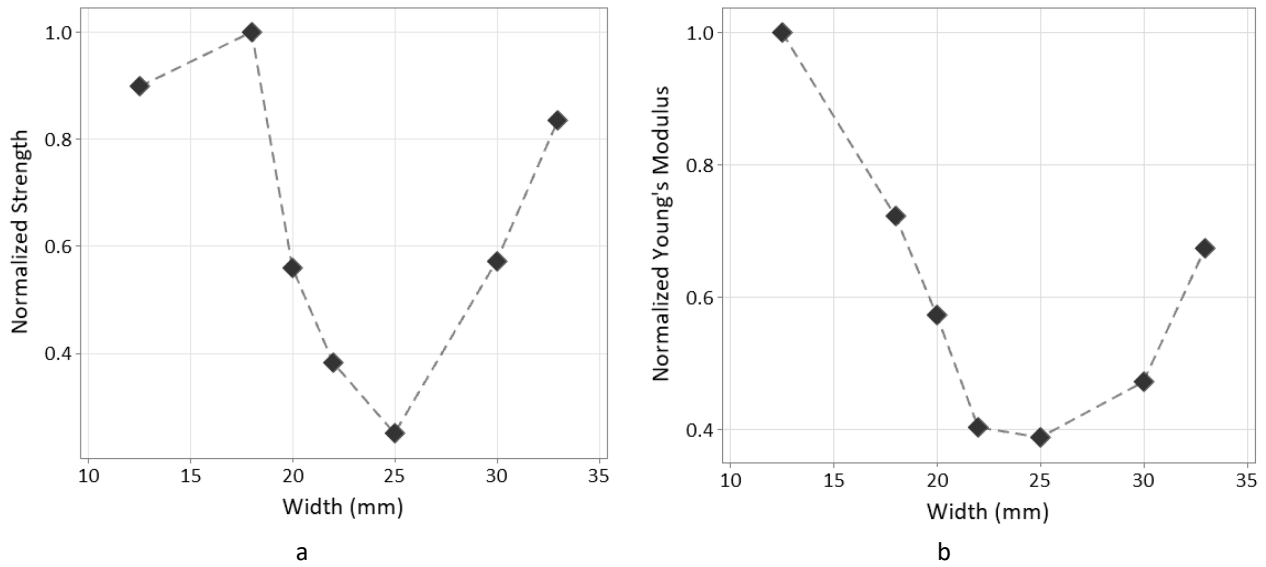
Figure 5. Results of the three-point bending test carried out on specimen at different widths. a) Normalized strength vs specimen width; b) normalized Young's modulus vs specimen width. Each point represents the average of the results for a specimen given dimension.

3.2 Tensile tests

Figure 6 shows the box plot of the tensile test results. The data are normalized according to the maximum strength and Young modulus value found in the batch of the tested specimen. Also in this case, the specimens with the prepreg density of 204 gr/m^2 performed better than the 600 gr/m^2 ones in terms of strength. The mean strength value of the 204 gr/m^2 specimen was 17% higher than the 600 gr/m^2 coupons. Strength confirmed to have high results dispersion: the normalized standard deviation was 0.203 for the 600 gr/m^2 specimens, and 0.13 for the 204 gr/m^2 specimens. Considering the stiffness, the difference in performance between the two densities is less marked: 204 gr/m^2 coupons had an 8% higher Young modulus respect to the 600 gr/m^2 specimens.
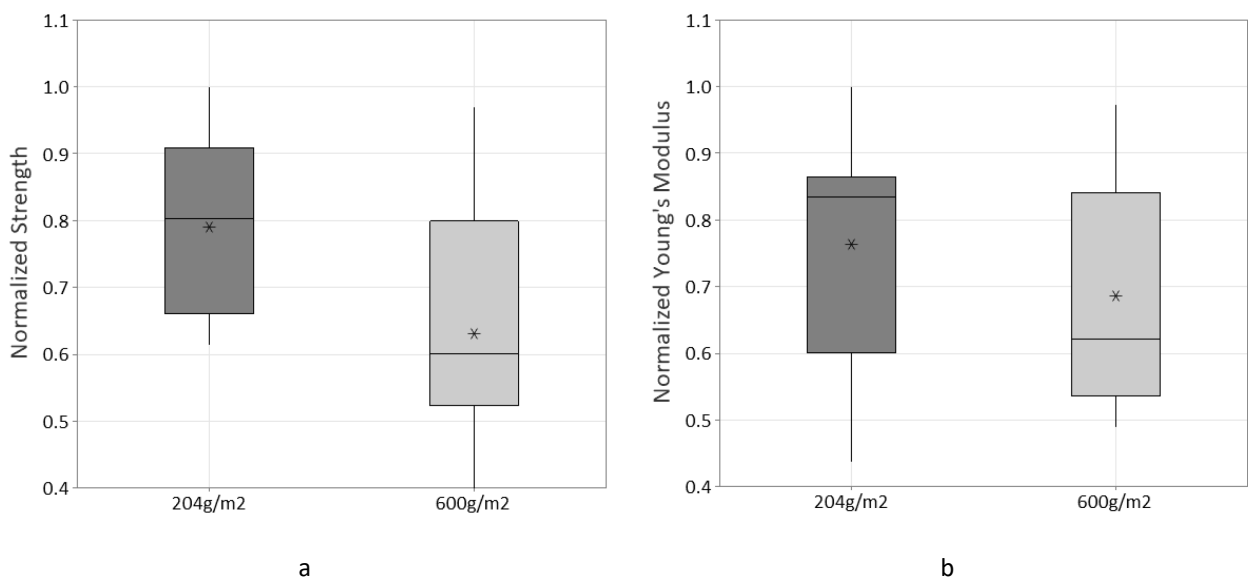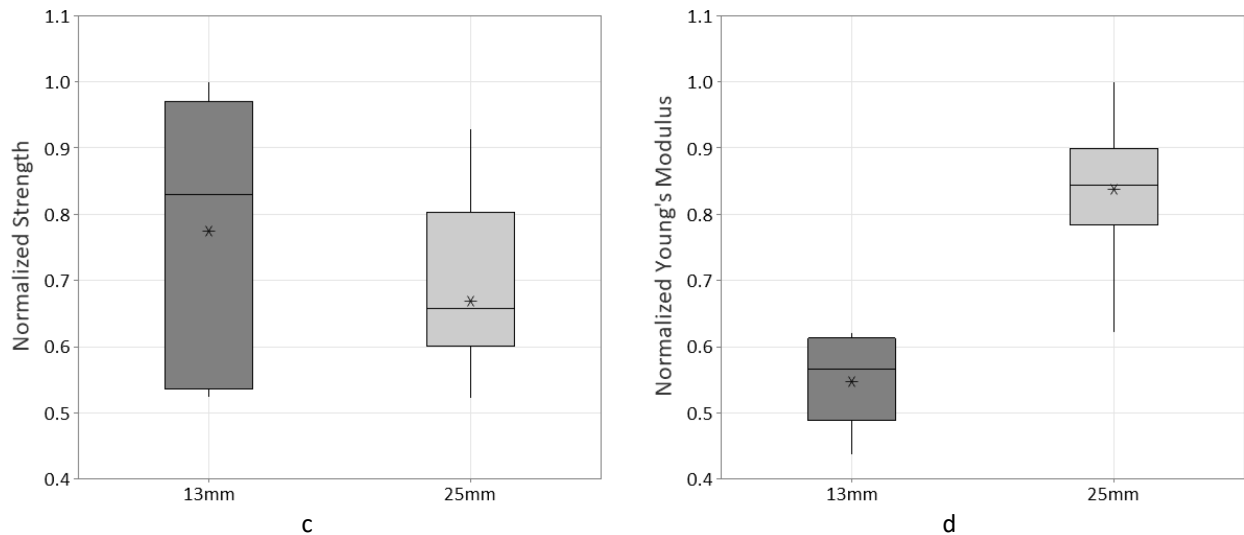
Figure 6. Box plot of the tensile test results. a) Normalized strength as function of the prepreg density; b) normalized Young's modulus as function of the prepreg density; c) Normalized strength as function of the specimen width; d) Normalized Young modulus as function of the specimen width.

Figure 7 shows the results of the tensile test in terms of normalized stress-strain. For clarity and readability, only some curves of the tested batch have been reported in the graph. Despite the dispersion, also in this case it is possible to group the results into 3 main categories, according to the failure type: 1) linear-elastic behavior until the ultimate stress and failure; 2) presence of one or more stress drops in the elastic phase, maximum stress, and failure; 3) linear-elastic phase followed by a "step-like" post-peak trend related to crack propagation. The stress values shown in figure 7 were normalized as a function of the maximum stress value measured in the tests. Each of these failure modes can be associated to a certain crack initiation, nucleation, and propagation.

Figure 8a shows the deformation map of the tested specimens, acquired through the DIC system. The behavior of type 1 is associated to a localized nucleation and propagation of the crack. As it can be seen from figure 8a, the maximum deformation region is restricted to the primary nucleation site: the fracture propagated transversally from the nucleation tip and extended between the two edges of the specimen.

In the case of type 2 small load drops were detected in the linear-elastic phase. During the test, some cracks and tips were audible, associated to the presence of secondary nucleation sites, i.e., regions where cracks initiated but did not cause the failure. Near to the edges of the central section of the specimen a secondary nucleation site is evidenced in figure 8a (highlighted by the white dashed box). The crack paths of the type 1 and 2 are shown in figure 8b. The crack followed the path of least resistance, passing through the interface regions and the rich resin areas. In this case, the chops were aligned along the thickness, leading the crack to easily propagate across the rich matrix areas.

Considering the type 3 behavior, the zones of maximum deformation were extended (figure 8a), and the specimen globally demonstrated a higher compliance than the type 1 and 2 behaviour. Multiple fractures generated in different portions of the specimen caused by the simultaneous presence of primary sites over a wide portion of the specimen surface. There was an extensive degradation of the properties, which generated a post-elastic load trend characterized by a plateau and load oscillations. Analyzing the fracture along the thickness, an extended step-wise crack path and chop debonding is noticeable (figure 8b). The crack propagation interfered with several resistance points, such as fibers oriented in different directions or interface regions. The crack-path was longer and discontinuous, generating the load fluctuations above mentioned. The final failure generally occurred by chop debonding, due to the interlaminar shear between the chops.
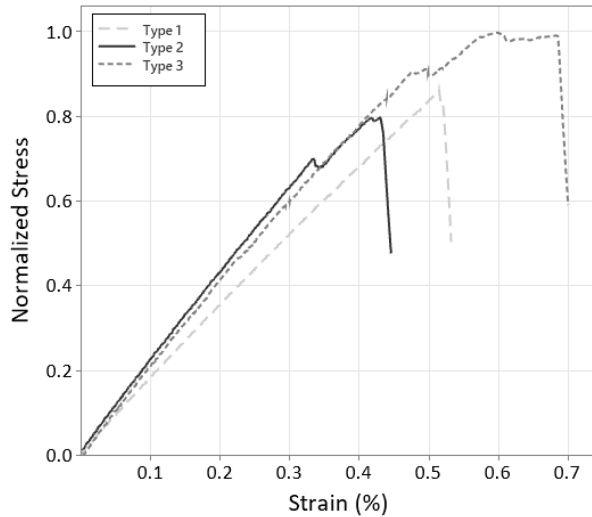
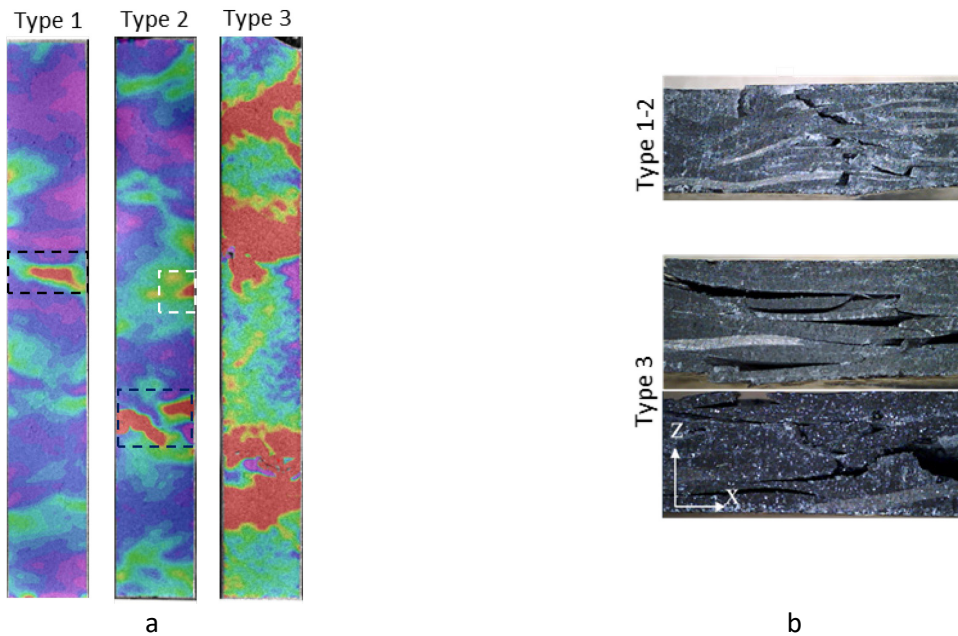Figure 7. Tensile test results. Normalized stress as function of the strain.

| a | b |

Figure 8. Fracture surfaces of the tensile specimens: a) strain map acquired with the DIC system; b) transversal fracture surfaces.

3.3 Application Study: accelerator pedal frame

This paragraph shows a preliminary result of the manufacturing an automotive component by means of the described technology. The component shown in Figure 9 represents an accelerator pedal frame of a Formula SAE vehicle. Figure 9a shows CAD of the component with dimension expressed in mm. The component was made with 20x20 mm chops, using the same process parameters described in paragraph 2.1. Although the presence of ribs and edges makes the component challenging to produce with this technology, the quality of the final product is remarkable. It is important to remark that the proposed element represents the first prototype produced, and different process and geometric parameters require several optimization cycles that will be deepened by the authors in future works. It is necessary to study the correct size of the cutouts, to guarantee a homogeneous filling of the mold, especially in correspondence of the ribs and the sharp edges. The mold temperature during the charge placement must be optimized to ensure that the chops sit well on the mold surfaces. The type of material to be used, the thickness and density must be properly designed according to the component to be produced. Indeed, although it has been shown by standard tests that the

prepreg with a surface weight density of 204 gr/m^2 turns out to be more performing, it has a smaller thickness. This implies to manage and handle a greater number of chops, making the mold charging procedure more intricate.
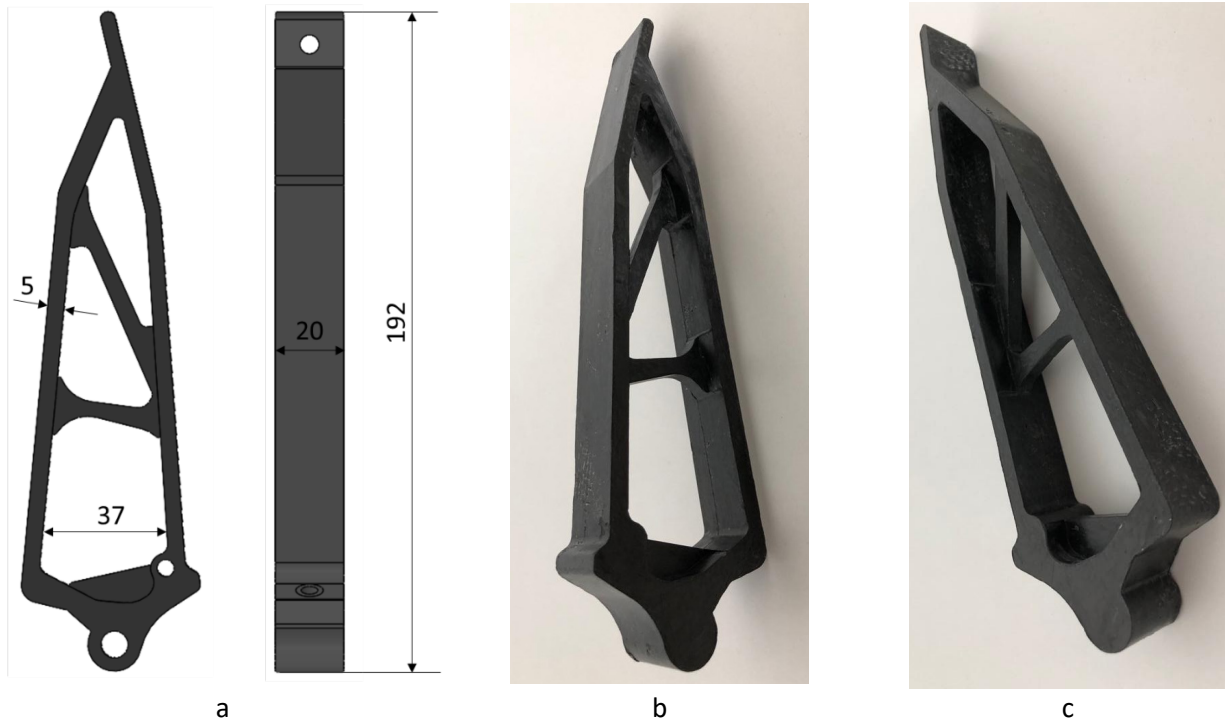

Figure 9. Prototype of an accelerator pedal frame produced with the PPMC technology: a) CAD model with basic dimensions expressed in mm; b-c) produced component

3.4 Discussion

The data analyzed in the previous sections showed a dispersion in the results and in the fracture modes, even within specimens belonging to the same batch. Contrary to non-oriented short-fiber composite materials, where the randomness of the fiber orientation makes the structure globally isotropic, in this type of structure the properties strongly depend on the local conditions of the material.

The main failure modes highlighted during the tests were found to be delamination, brittle fracture of the matrix, fracture of the interface regions and debonding between the chops. During the mechanical tests, the failure generally occurred as an interaction between all these fracture modes. The material generates simultaneously several fracture precursors sites where the crack propagated. The coexistence of primary and secondary crack nucleation sites was found on several specimens tested in traction. Primary sites nucleated at the specimen's edge where the chop size is reduced due to the cutting process. Edge regions are thus weaker than the central portion of the specimen, where the chops keep their nominal dimension.

The occurrence of one of the types of fracture above highlighted may seem a purely stochastic event and not predictable a priori, even if analyzing the stacking path of the chops it is possible to move towards a more deterministic approach.

The crack tends to propagate towards the areas of least resistance, which in the analyzed material are represented by the interface regions. Aligned interface regions along the thickness (figure 10a) lead the crack to pass through them, following a shorter path. On the contrary, if the chops are stacked with a greater overlap (figure 10b), the interface regions are less aligned, and consequently the crack run across a longer

and tortuous path, faces more resistance zones, and the global load carrying capability of the specimen increases.

The specimens with a prepreg density of 600 gr/m^2 showed lower strength than the specimens with a prepreg density of 204 gr/m^2. The 600 gr/m^2 and 204 gr/m^2 prepregs have a thickness respectively of 0.6 mm and 0.3 mm. Consequently, the 600 gr/m^2 specimens will have a lower number of chops along the thickness than the 204 gr/m^2 specimens. A smaller number of chops along the thickness means a lower probability for the crack to face propagation resistance spots, and consequently these specimens are characterized by a lower mechanical strength.
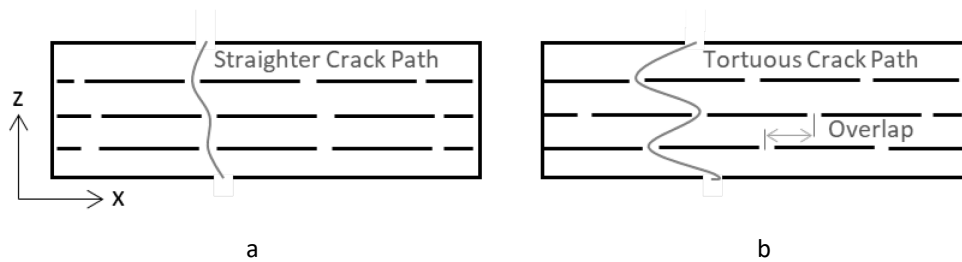

a   b

Figure 10. Crack propagation paths. a) transversally aligned chops; b) overlapped chops.

Conclusion

A methodology for the in-line production scraps recovery of bidirectional carbon fiber prepreg was here presented. The production of stochastic prepreg platelet molded composites with out of autoclave technology makes the material desirable for mass production applications due to its simplicity and cost-effectiveness.

An experimental test campaign of material characterization was carried out. The three-point bending, and tensile tests have shown scattered results in terms of stiffness and strength, due to the interaction of different failure modes. This dispersion is however limited to three different failure modes, that are triggered according to the meso-structure of the component. The interface between the chops has a significant influence on the mechanical response. Prior to the failure, several damage nucleation sites occurred, generally at chop interface. Delamination, brittle fracture of the matrix and chop debonding are the primary failure modes.

A relationship between the chop dimension and the specimen size in bending was evidenced too. The failure mode goes from interface cracking to chop fiber rupture as a function of the specimen width. This is due to the high heterogeneity of the material, that is emphasized for smaller specimens. This aspect is of paramount importance considering the perspective of manage the material mechanical response as a function of the target application and will be enhanced in future works.

The effect of the prepreg thickness was analyzed. Thinner prepreg demonstrated to perform better than thicker prepreg. Indeed, thinner prepreg implies a greater number of stacked chops over the material's thickness, leading the crack to come across several resistance-propagation spots.

In conclusion, the mechanical properties are confirmed to be suitable for a potential semi-structural use, and the benefits in terms of light weighting, waste recovery and cost reduction makes this technology interesting for automotive applications and therefore further deeper investigations will be performed.

Bibliography

[1]   Koumoulos EP, Trompeta A, Santos R, Martins M, Iglesias V, Böhm R, et al. Research and Development in Carbon Fibers and Advanced High-Performance Composites Supply Chain in Europe : A Roadmap for Challenges and the Industrial Uptake 2019.

[2]   European Parliament and Council. Directive 2000/53/EC on end-of-life vehicles. Official Journal of the European Union 2000;L:34–42.

[3]   Bledzki AK, Seidlitz H, Goracy K, Urbaniak M. Recycling of Carbon Fiber Reinforced Composite Polymers — Review — Part 1 : Volume of Production , Recycling Technologies , Legislative Aspects 2021.

[4]   Perspectives F. and Future Perspectives 2021:1–13.

[5]   Snudden JP, Ward C, Potter K. Reusing automotive composites production waste. Reinforced Plastics 2014;58:20–7. https://doi.org/10.1016/S0034-3617(14)70246-2.

[6]   Meng F, Mckechnie J, Turner T, Wong KH, Pickering SJ. fibre composites in automotive applications Environmental aspects of use of recycled carbon fibre composites in automotive applications 2017. https://doi.org/10.1021/acs.est.7b04069.

[7]   Adekomaya O. Adaption of green composite in automotive part replacements : discussions on material modification and future patronage 2020.

[8]   Pimenta S, Pinho ST. Recycling carbon fibre reinforced polymers for structural applications : technology review and market outlook 2010:378–92. https://doi.org/10.1016/j.wasman.2010.09.019.

[9]   Liu B, Zhu P, Xu A, Bao L. Investigation of the recycling of continuous fiber-reinforced thermoplastics. Journal of Thermoplastic Composite Materials 2019;32:342–56. https://doi.org/10.1177/0892705718759388.

[10]   Wan Y, Takahashi J. Development of Carbon Fiber-Reinforced Thermoplastics for Mass-Produced Automotive Applications in Japan. Journal of Composites Science 2021;5:86. https://doi.org/10.3390/jcs5030086.

[11]   Tapper RJ, Longana ML, Hamerton I, Potter KD. A closed-loop recycling process for discontinuous carbon fibre polyamide 6 composites. Composites Part B: Engineering 2019;179:107418. https://doi.org/10.1016/j.compositesb.2019.107418.

[12]   Boria S, Belingardi G, Fiumarella D, Scattina A. Experimental crushing analysis of thermoplastic and hybrid composites. Composite Structures 2019;226:111241. https://doi.org/10.1016/j.compstruct.2019.111241.

[13]   Feraboli P, Peitso E, Deleo F, Cleveland T, Stickler PB. Characterization of prepreg-based discontinuous carbon fiber/epoxy systems. Journal of Reinforced Plastics and Composites 2009;28:1191–214. https://doi.org/10.1177/0731684408088883.

[14]   Kravchenko SG, Sommer DE, Denos BR, Favaloro AJ, Tow CM, Avery WB, et al. Tensile properties of a stochastic prepreg platelet molded composite. Composites Part A: Applied Science and Manufacturing 2019;124:105507. https://doi.org/10.1016/j.compositesa.2019.105507.

[15]   Selezneva M, Lessard L. Characterization of mechanical properties of randomly oriented strand thermoplastic composites. Journal of Composite Materials 2016;50:2833–51. https://doi.org/10.1177/0021998315613129.

[16]   Visweswaraiah SB, Selezneva M, Lessard L, Hubert P. Mechanical characterisation and modelling of randomly oriented strand architecture and their hybrids – A general review. Journal of Reinforced Plastics and Composites 2018;37:548–80. https://doi.org/10.1177/0731684418754360.

[17]   Feraboli P, Cleveland T, Stickler P, Halpin J. Stochastic laminate analogy for simulating the variability in modulus of discontinuous composite materials. Composites Part A: Applied Science and Manufacturing 2010;41:557–70. https://doi.org/10.1016/j.compositesa.2010.01.003.

[18]   LeBlanc D, Landry B, Levy A, Hubert P, Roy S, Yousefpour A. Compression moulding of complex parts using randomly-oriented strands thermoplastic composites. International SAMPE Technical Conference 2014.

[19]   Nilakantan G, Nutt S. Reuse and upcycling of thermoset prepreg scrap: Case study with out-of-autoclave carbon fiber/epoxy prepreg. Journal of Composite Materials 2018;52:341–60. https://doi.org/10.1177/0021998317707253.

[20]   Ko S, Yang J, Tuttle ME, Salviato M. Effect of the platelet size on the fracturing behavior and size effect of discontinuous fiber composite structures. Composite Structures 2019;227:111245. https://doi.org/10.1016/j.compstruct.2019.111245.

[21]   Belingardi G, Boria S, Scattina A. Delaminazione Sperimentale E Numerica in Laminati. Sperimentale 2011:7–10.

[22]   Davidson BD, Sundararaman V. A single leg bending test for interfacial fracture toughness determination. International Journal of Fracture 1996;78:193–210. https://doi.org/10.1007/BF00034525.